1985

Computer-simulated energy and angular distributions of sputtered Cu atoms

Shapiro, M.H.; Haff, P.K.; Tombrello, T.A.; Harrison, D.E., Jr.; Webb, R.P.

Taylor & Francis Online

Shapiro, M. H., et al. "Computer-simulated energy and angular distributions of sputtered Cu atoms." Radiation effects 89.3-4 (1985): 243-255.
http://hdl.handle.net/10945/61421

Radiation Effects, 1985, Vol. 89, pp. 234–255
0033-7579/85/8904-0243$18.50/0

COMPUTER-SIMULATED ENERGY AND ANGULAR DISTRIBUTIONS OF SPUTTERED Cu ATOMS

M. H. SHAPIRO
Department of Physics, California State University, Fullerton, Fullerton, California 92634
and
Division of Physics, Mathematics, and Astronomy, Caltech, Pasadena, California 91125

P. K. HAFF and T. A. TOMBRELLO
Division of Physics, Mathematics, and Astronomy, Caltech, Pasadena, California 91125

and

D. E. HARRISON, Jr. and R. P. WEBB†
Department of Physics, Naval Postgraduate School, Monterey, California 93943

(*Received December 5, 1983; in final form August 15, 1984*)

The energy and angular distributions of copper atoms ejected by 5 keV incident Ar ions have been simulated using the multiple interaction molecular dynamics technique. Calculations carried out with two independently written computer codes yielded essentially identical results. As in previous simulation studies of low to medium energy sputtering, virtually all ejected atoms came from the first layer or second layer. Two different ion–atom potentials were used in the simulations. Absolute sputtering yields depended strongly on the choice of potential; relative yields and angular distributions were found to be insensitive to the choice of potential. For Ar ions normally incident on the (100), (110), and (111) faces of a fcc Cu crystallite, ejected atoms from the second layer of the crystallite exited preferentially in the forward direction compared to those sputtered from the first layer. The energy spectra of atoms ejected from the second layers were harder than those of the first layer atoms.

1 INTRODUCTION

Until recently it was not possible to determine experimentally the origin of material sputtered by low to medium energy ion beams. However, new measurements by Dumke[1,2] of the sputtering of a liquid gallium–indium eutectic alloy by Ar ions at 15 and 25 keV provide direct evidence that a large fraction of sputtered atoms arise from the first target layer. In addition, at 15 keV Dumke's results indicated that atoms from the second layer were emitted preferentially in the direction of the normal to the target surface. These experimental observations have prompted us

†Present Address: Department of Electronics and Electrical Engineering, University of Surrey, Guildford, Surrey, GU2 5XH, England.

to carry out computer simulations on simpler systems aimed at determining the energy and angular distributions of particles ejected from different layers of a target.

For this investigation the Ar–Cu system was chosen because of the ready availability of well-studied potentials and the wealth of available experimental data. Previous work by Harrison[3] and Harrison and Webb[4] has shown that, except for absolute yields, the features of the ejection processes are almost independent of the choice of potential parameters. The results obtained in this study confirm that observation. For reasons of computational economy a bombarding energy of 5 keV was chosen for the incident Ar^+ ion. This energy is near the maximum in the experimental yield curves[5,6] for Ar ions incident on monocrystalline Cu, and relatively small (400 to 500 atom) crystallites are adequate for the accurate calculation of the distributions of interest.[7] The low incident energy and small crystallite size both tend to minimize the amount of computer time required to generate the necessary spectra. Simulations were carried out using two independently written computer codes in order to provide a cross-check on the results.

2 COMPUTER CODES AND POTENTIAL FUNCTIONS

One series of calculations was carried out using the QRAD code developed by the Naval Postgraduate School group, while another series was carried out using a code written by the CSUF-Caltech group. The NPS code written by Harrison and collaborators has been in use for many years, and has been described in previous papers.[8,9] It employs an "average force" algorithm[10] for the integration of the equations of motion in Hamiltonian form. The code is written in FORTRAN and was run on the IBM3033 computer at the Naval Postgraduate School.

The CSUF-Caltech code "SPUT1" was written for the California State University Data Center Cyber-760 system. SPUT1 employs a conventional predictor–corrector algorithm for the integration of the equations of motion in Newtonian form. To enhance calculational speed only a low-order corrector is used. The time-step is adjusted to keep the predictor and corrector within a chosen accuracy limit. After each successful time-step integration, the time-step is increased by 10%. If during any time-step the velocity corrector exceeds the velocity predictor by the chosen error limit, the time-step is halved and the calculation for that step is done again. The SPUT1 program is described in more detail in Ref. 11.

The results reported in this paper were obtained with the SPUT1 code. However, in several cases comparisons were made with relative yields, enregy spectra, and angular distributions produced by QRAD for the same initial conditions. Quantitative agreement was obtained to within a few percent for relative yields. Energy spectra and angular distributions produced by the two codes also showed very good agreement. The fine structure on the high energy side of the main peaks in the energy distributions (see Figures 1a, 1b, 2a, and 2b) were produced by both codes.

Complete verification of lengthy and complicated computer codes often is not possible. The SPUT1 code was written with different internal logic to provide an independent check on the existing codes. Our results provide evidence that no significant programming errors remain in either QRAD or SPUT1.

The interaction between atoms in the Cu lattice was represented by a composite pair potential. This pair potential function consists of three parts: a repulsive Born–Mayer potential at small distances, an attractive Morse potential at larger distances, and a cubic spline which provided a smooth transition between the two.

The composite potential between any pair of atoms in the lattice thus had the form

$$V_{ij} = A\exp(-BR), \quad R < R_a$$

$$V_{ij} = C_0 + C_1R + C_2R^2 + C_3R^3, \quad R_a \leqslant R < R_b$$

$$V_{ij} = D_e\exp[-\beta(R-R_e)]\{\exp[-\beta(R-R_e)]-2\}, \quad R_b \leqslant R < R_c$$

$$V_{ij} = 0, \quad R \geqslant R_c.$$

The parameters used with this potential function are given in Table I. They are essentially the same as those used by Garrison, Winograd, and Harrison.[12] However, the coefficients of the cubic spline were recomputed with a high precision fitting routine. This resulted in minor changes in these coefficients. The new spline joins more smoothly to the other two potential segments.

TABLE I

Potential parameters

Cu–Cu

A	B	C_0	C_1	C_2	C_3	D_e	β	R_e	R_a	R_b	R_c
(keV)	(Å^{-1})	(eV)	(eV/Å)	(eV/Å^2)	(eV/Å^3)	(eV)	(Å^{-1})	(Å)	(Å)	(Å)	(Å)
22.564	5.088	588	−853.0	428.0	−72.0	0.48	1.405	2.628	1.500	1.988	4.338

Ar–Cu (B-potential)

A	B
(keV)	(Å^{-1})
71.303	4.593

Ar–Cu (R-potential)

A	B
(keV)	(Å^{-1})
59.874	7.200

For the Ar–Cu interaction, a standard Born–Mayer repulsive potential with a radial cut-off was used. This has the form

$$V_{ij} = A\exp(-BR), \quad R < R_a,$$

$$V_{ij} = 0, \quad R \geqslant R_a.$$

Two sets of parameters were used with this potential function (see Table I). One set, the KSE or "B" potential,[13] corresponds to a relatively "large" radius for the incident ion and is more appropriate for the Au/Sb^+ system; while the other, the "Harrison-*R*" potential, corresponds to a relatively "small" radius.[3] Large target absolute yields produced by simulations with the *R*-potential are very close to the experimental yields. With the smaller targets used in our simulations absolute yields are underestimated, but relative yields compare favorably with experimental results. The use of two different potential choices in the simulation allows us to determine the sensitivity of the calculations to changes in the potential function. In addition, these particular choices bracket essentially all different ion–atom potentials that have been used to investigate the Cu/Ar^+ system.[3] Except for absolute yields, the choice of ion–atom potential had little effect on the results obtained from these simulations. The parameters for both ion–atom potentials are included in Table I.

3 RESULTS

A. *Yields*

Generally, the simulations reported in this paper were done with crystallites which had surface areas of 7 lattice constants by 7 lattice constants (25.1 Å × 25.1 Å). Crystallites which were 4 atomic layers thick (400 to 500 atoms) were used for the (100) and (111) orientations. For the (110) orientation 6 layer crystallites were used in order to have targets of approximately the same physical dimensions for all orientations. No edge or corner atoms were included in yields or angular distributions since their binding energies are artificially low. To approach full containment at 5 keV requires the use of much larger targets. Typically, 8 layer crystallites with 2000 or more total target atoms would be needed.[7] Studies with targets of this size produce yields that are quite close to experimental values for the *R*-potential. The *B*-potential yields are too large by a factor of 3 for the same size targets (Harrison, private communication). A general discussion of the containment problem is given in Ref. 14. In particular, it is shown there that the ratio of yields from different crystal orientations is almost independent of target size for targets exceeding about 200 atoms.

For 5 keV Ar ions normally incident on monocrystalline Cu targets, the experimentally observed yields are about 4.1 for the (100) face, 2.7 for the (110) face and 9.4 for the (111) face.[5,6] The experimental relative yields for the three faces thus are in the ratio 1.5:1.0:3.5. The relative yields obtained from the *R*-potential simulations were in the ratio 1.6:1.0:3.3 which is in excellent agreement with the experimental data. Relative yields obtained from the *B*-potential simulations are (1.5: 1.0:1.6) indicating that the (100) and (110) contributions were overestimated because the large ion reduces the effect of channeling.

For both the *R*-potential and *B*-potential simulations, we found that essentially all ejected atoms originated from the first or second layer of the target. In the case of the *B*-potential simulations the yields arising from the first layer comprised 85%, 67%, and 92% of the total for the (100), (110), and (111) orientations, respectively, while the corresponding yields arising from the second layer were 13%, 28%, and 7%. For the *R*-potential simulations corresponding first layer yields comprised 91%, 75%, and 92% of the total, while the second layer yields were 9%, 21%, and 8%. For both choices of ion–atom potential the most open orientation (110) produced

TABLE II
Yield results

Orientation	*B*-potential				*R*-potential				Experimental[a]	
	Layer 1	Layer 2	All	Ratio	Layer 1	Layer 2	All	Ratio	All	Ratio
(100)	9.84	1.49	11.55	1.5	2.30	0.22	2.54	1.6	4.1	1.5
(110)	5.32	2.24	7.91	1.0	1.15	0.33	1.54	1.0	2.8	1.0
(111)	11.57	0.89	12.63	1.6	4.63	0.38	5.05	3.3	9.5	3.4

[a]Experimental results are an average of the data reported in Refs. 5 and 6.

the largest fraction of second layer yield. However, it should be noted that in our simulations we have assigned to the "first layer" only those atoms having their centers initially in the surface layer of the crystallite. In the case of the (110) orientation, there is considerable overlap of first and second layer atoms. A complete summary of our yield results is given in Table II.

The statistical uncertainties in the yields and yield ratios were estimated by repeating several runs with the same program parameters except for the random number seed. In SPUT1 the target impact area, which reflects the basic symmetry of the crystal face, is broken into 100 sub-areas. The sub-areas are scanned uniformly, but within the sub-areas impact points are determined randomly. The standard deviation of the yields from these repeated runs was approximately half that expected from counting statistics. On this basis, we estimate that the statistical uncertainty in the yields is less than 2 or 3%. Likewise, the uncertainty in ratios of yields is about 5%.

B. *Ejected Atom Energy Distributions*

Figure 1a shows the energy distribution of *all* Cu atoms ejected by 200 Ar impacts on the (100) face of a Cu crystallite that had dimensions of 7×7 lattice constants and was 4 layers thick. These data were collected in 1-eV wide bins. With this bin size the distribution peaks at about 2.5 eV and decreases rapidly at higher energies. However, a substantial high energy tail is present which extends to energies beyond 100 eV. Figures 1b and 1c show the energy spectra for those ejected atoms arising from the first layer of the crystallite and from the second layer respectively. Comparison of the two spectra reveals that the second layer spectrum has a greatly reduced low-energy component. In Figure 1 results obtained with the *R*-potential are shown with solid lines, while *B*-potential results are shown with dashed lines.

While the yields are lower for the *R*-potential, the basic conclusion remains the same. The second layer ejected atom spectrum has a greatly reduced low-energy component. Similar results were obtained for simulations with the target crystallite in the (111) orientation (Figures 2a–2c, solid lines). For the (110) orientation, which is less densely packed, the energy spectrum from the second layer (Figures 2a–2c, dashed lines) shows a larger low-energy component than the other two orientations. However, even in this orientation, the second layer energy spectrum is relatively much harder than the first layer spectrum.

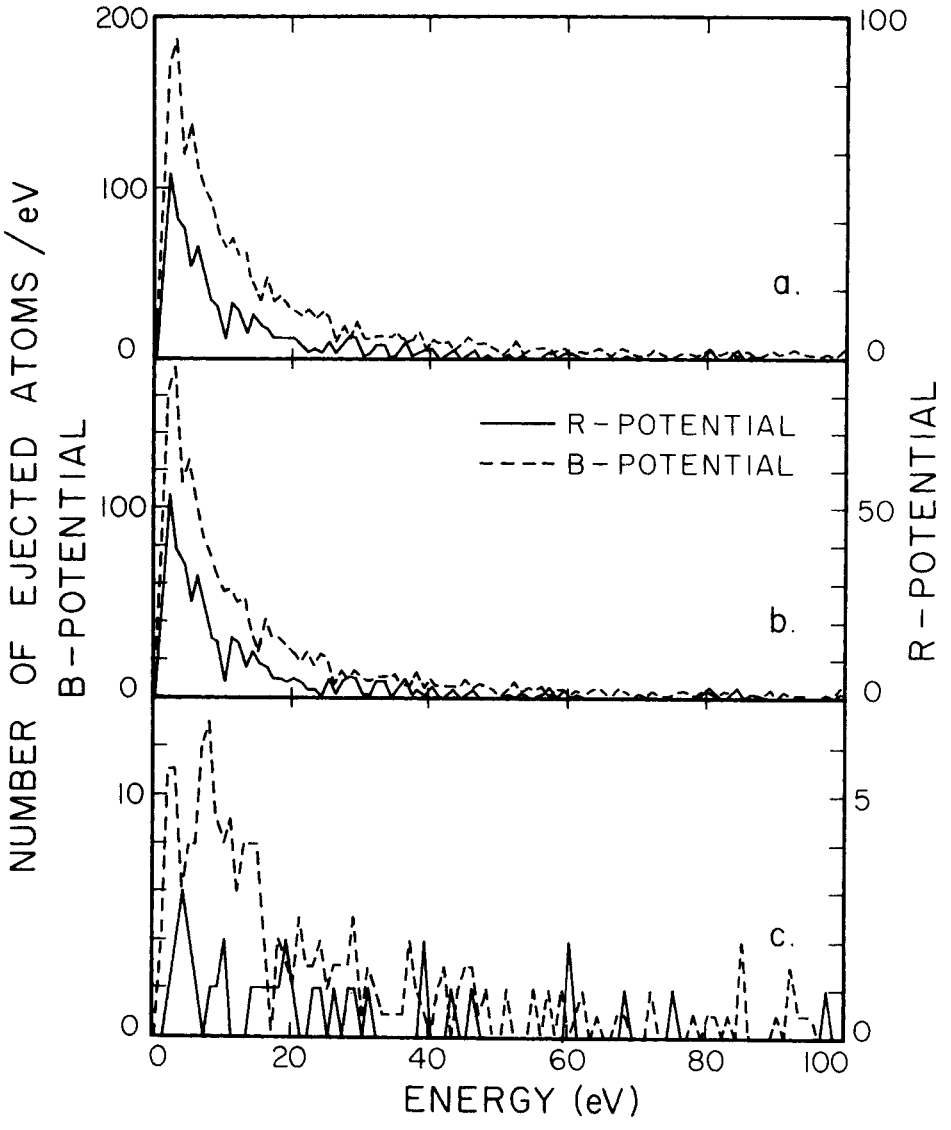

FIGURE 1 Energy spectra obtained from a simulation with 200 Ar^+ ions normally incident on the (100) face of a Cu crystallite. (a) All ejected atoms, (b) first layer ejected atoms only, (c) second layer ejected atoms only. *R*-potential results are shown with the solid line, while *B*-potential results are shown dashed.

Transport theory[15] predicts that the shape of the energy distribution should follow a function of the form

$$N(E) = AE/(E+E_b)^n,$$

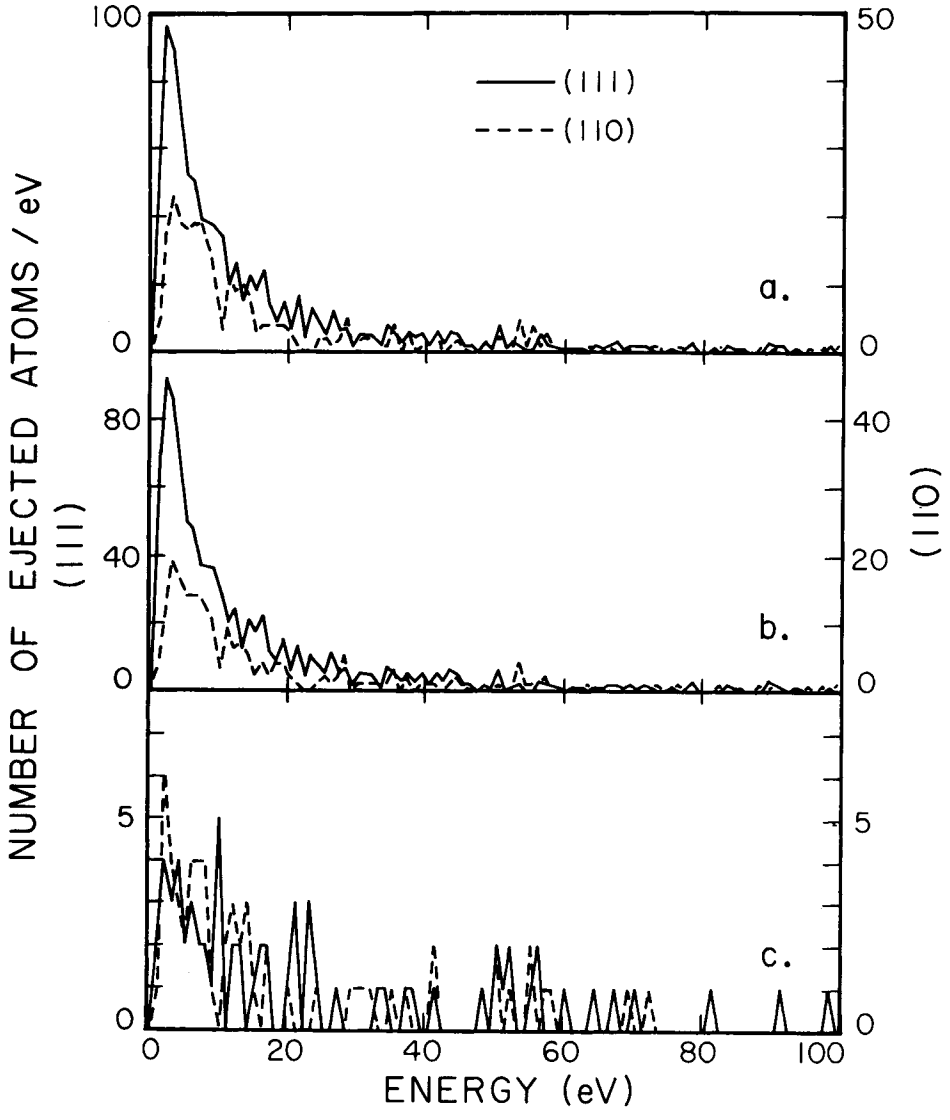

FIGURE 2 Spectra similar to those in Figure 1, except from the (111) face of copper (solid lines) and (110) face (dashed lines). For both crystal orientations only R-potential results have been plotted.

where A is a parameter independent of energy, E_b is the surface binding energy, and n is equal to 3 for hard sphere scattering. On the tail of the energy distribution, this leads to the well known E^{-2} shape. For each crystal orientation and for each choice of potential, we have determined the parameters A, E_b and n which produced the best fit to the energy spectrum of atoms ejected from all crystallite layers by minimizing χ^2. This minimization was carried out in two stages. First, contours

TABLE III
Energy spectra parameters

Ion–atom potential	Crystal orientation	A	n	E_b (eV)	χ^2/deg. of freedom
B	(100)	37,425	3.13	5.21	1.84
B	(110)	23,000	3.20	5.63	2.94
B	(111)	61,062	3.34	4.72	2.12
R	(100)	9,081	3.21	4.56	1.12
R	(110)	2,700	3.00	5.08	1.03
R	(111)	33,250	3.40	5.12	1.44

of χ^2 values were determined for a wide range of values of the independent variables. Then an automatic search program was used to locate the minimum in the χ^2 hypersurface. In the second stage the range of independent variables was limited to the vicinity of the minimum found in the first stage. To check the ability of the program to find the minimum correctly, the search was repeated with different starting points. In all cases the final values of the parameters were located to within the minimum step size of the search program. The results are summarized in Table III.

In general, the energy spectra produced by simulations with the *R*-potential were fitted best with values of n near 3 and values of E_b near 4.7 eV. Fit quality was better for the *R*-potential spectra than for the *B*-potential spectra. The data of Farmery and Thompson[16] for 40 keV Ar^+ ions incident on monocrystalline copper generally follow the E^{-2} distribution for all crystal orientations. Our energy spectra are consistent with this result.

The values of E_b found from fitting the energy spectra are reasonably consistent with Jackson's calculations[17] of this parameter for Cu. (E_b depends on crystal orientation.[17]) The sample size for energy spectra produced in our simulations, however, is insufficient to distinguish meaningfully between the values of E_b obtained for the various orientations.

C. *Angular Distributions*

Perhaps the most striking difference between the first and second layer ejected atom populations is the very different polar angular distributions of the sputtered atoms. Figure 3a shows the polar angular distribution of all ejected particles resulting from 200 impacts on a crystallite oriented in the (100) direction with the *B*-potential (dashed line). (These angular distributions represent the number of ejected atoms per unit solid angle averaged over all azimuthal angles. The normal to the crystallite surface is at zero degrees.) Similar results for the *R*-potential also are shown in Figure 3a (solid lines) In both cases the angular distributions are fairly broad, with substantial yields out to 50 degrees and beyond.

Polar angular distributions for particles ejected from the individual layers are shown in Figures 3b and 3c. For both choices of potential, the polar angular distributions for first layer ejected atoms are broad, with some peaking near 45 degrees. On the other hand, second layer ejected atoms are directed strongly towards the normal to the target face. While some yield remains out to 50 degrees, much of the yield is concentrated about the normal to the target.

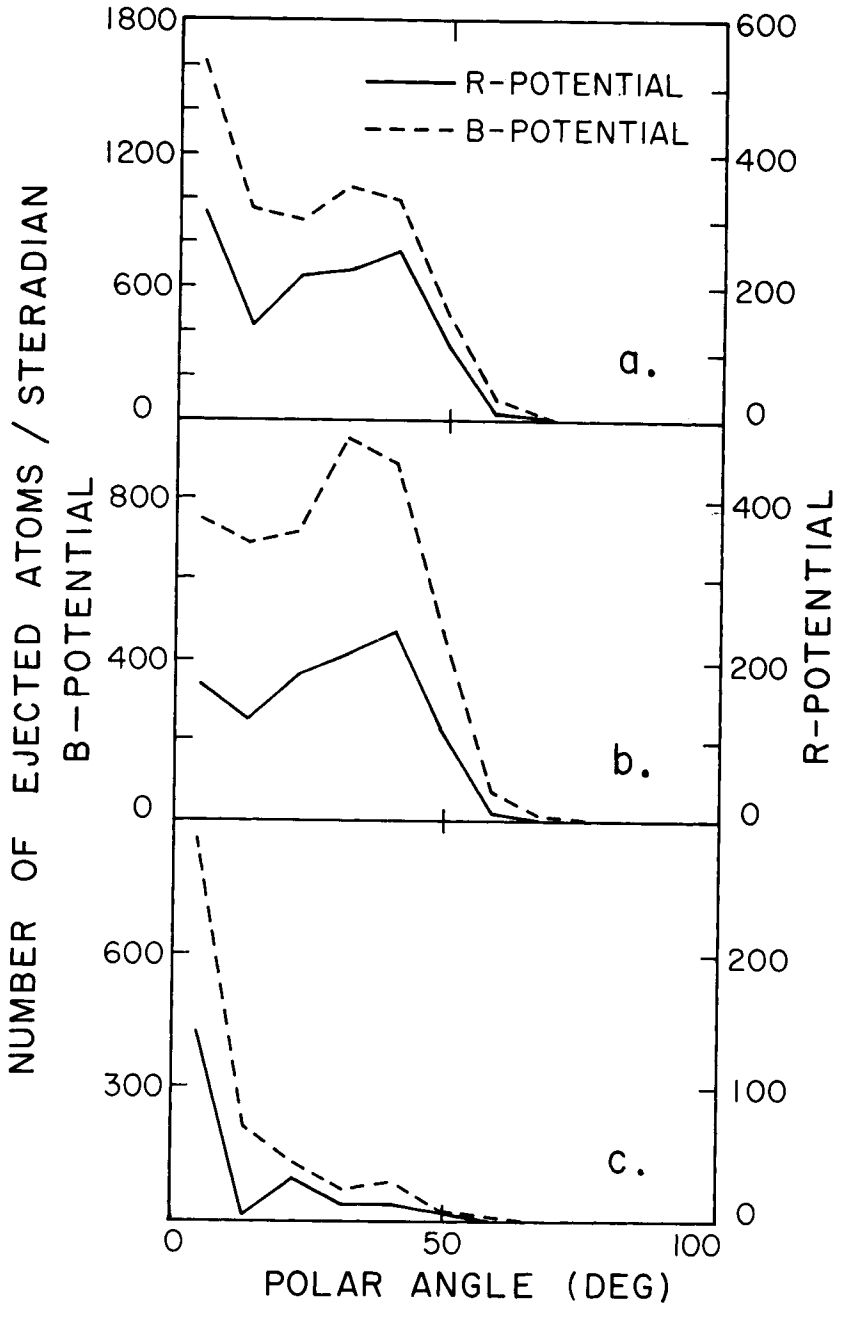

FIGURE 3 Polar angular distributions of ejected particles obtained from a simulation with 200 Ar^+ ions normally incident on the (100) face of a Cu crystallite. (a) All ejected atoms, (b) first layer ejected atoms only, (c) second layer ejected atoms only. *R*-potential results are shown with solid lines, *B*-potential results are shown dashed.

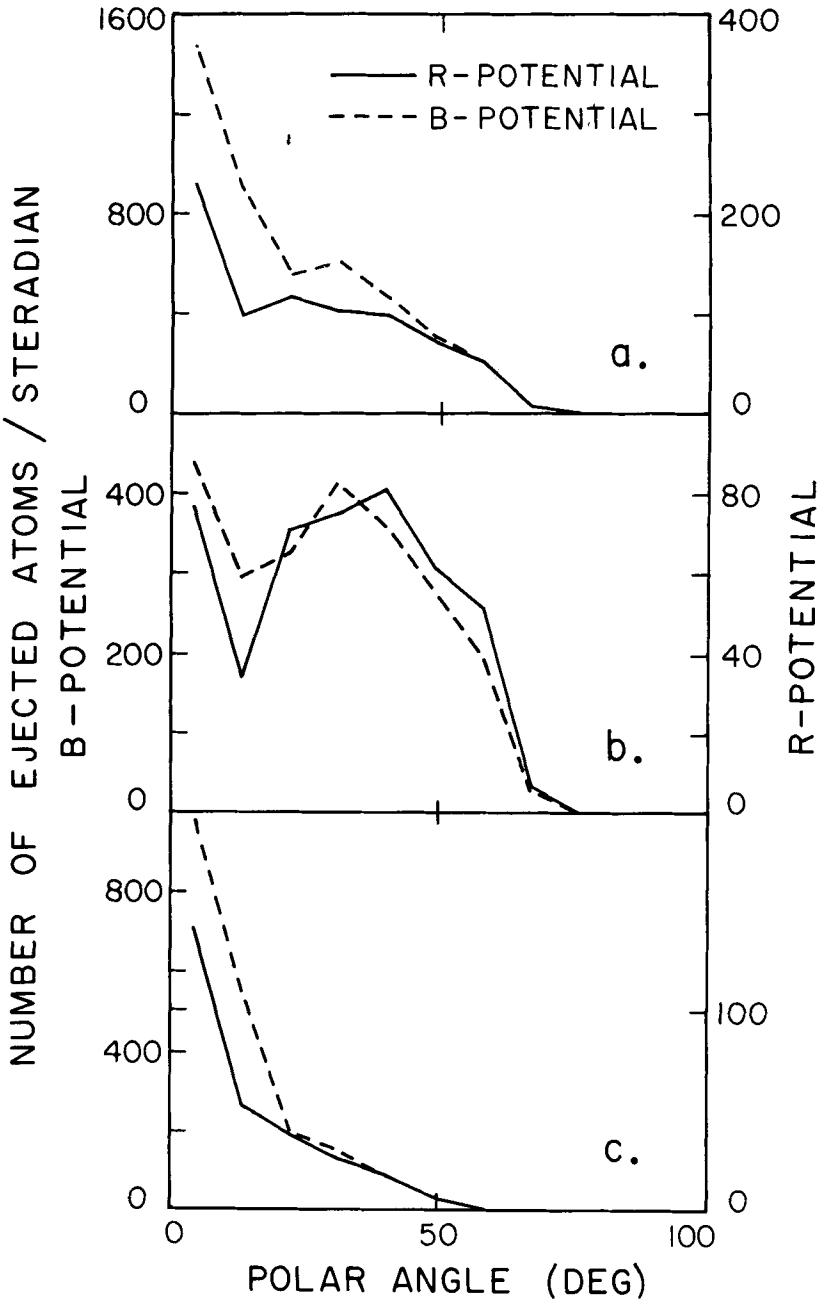

FIGURE 4 Polar angular distributions similar to those in Figure 3 except from the (110) fac of Cu. (*R*-potential solid, *B*-potential dashed.)

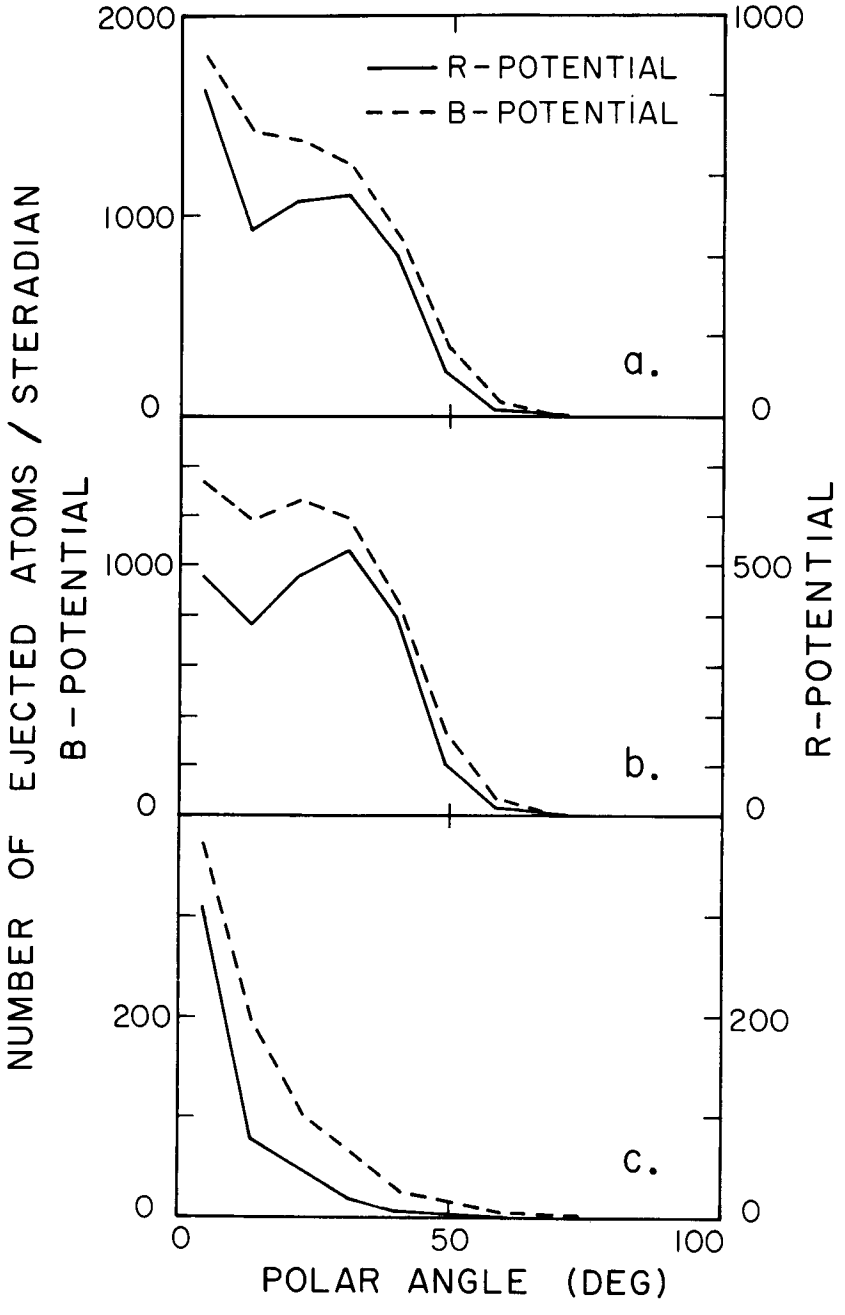

FIGURE 5 Polar angular distributions similar to those in Figure 3 except from the (111) face of Cu. (*R*-potential solid, *B*-potential dashed.)

Similar results are found for the other two crystallite orientations. (110) data are shown in Figures 4a–4c, while (111) data are shown in Figures 5a–5c. In all cases the basic trends are the same. The polar angular distributions of second layer ejected atoms are more forward peaked than those of the first layer ejected atoms.

The azimuthal angular distributions generally retain the symmetry of the target crystal face. Thus comparison of the angular distributions shown in Figures 3 through 5 with experimental data would require suitable summation of the experimental data about the polar axis. Unfortunately, at this time there is a paucity of quantitative experimental data available which can be analyzed in this way.

4 DISCUSSION

The results obtained from these simulations suggest that atoms ejected from the second layer of single crystal targets by normally incident beams are emitted preferentially in the normal direction, while those ejected from the first layer have a much broader polar angular distribution. In addition, the energy spectrum of ejected atoms from the second layer is harder than that of ejected atoms from the first layer. These results are largely independent of crystal orientation.

A detailed examination of the atoms ejected by each individual incident Ar ion revealed that second layer sputtered atoms seldom were ejected by themselves. Events which produced second layer ejected atoms also produced a number of first layer ejected atoms. The ejection of first layer atoms produces "holes" through which second layer ejected atoms can exit.[19] This explains the similarity in polar angular distributions for (100), (110), and (111) orientations of the crystallite. For the (110) orientation which is relatively open, the pre-existing holes in the first layer are large and the corresponding ratio of second layer to first layer ejected atoms is greatest for this orientation.

Comparison of the energy spectra of the second layer ejected atoms with energy spectra of first layer ejected atoms showed that the large low energy peak near 2.5 eV is present only for first layer ejected atoms. The second layer energy spectra in all cases resembled the high-energy tail of the first layer distribution. We interpret this result to imply that several additional eV are expended by second layer ejected atoms in crossing the first layer of atoms.

These results also suggest that only a small subset of possible collision mechanisms between the incident Ar ion and the Cu lattice transfer the necessary momentum transverse to the beam direction to eject a second layer (or deeper) atom. While many atoms from deeper layers may acquire momentum towards the surface, they are not likely to have enough energy to cross the surface layer. However, in many cases a replacement collision with an atom in the surface layer would transfer enough momentum to eject a surface layer atom. This would explain the predominance of first layer sputtering, since more classes of collision mechanisms would be able to transfer the relatively small normal momentum needed for excape.

In some circumstances it may be possible to take advantage of these observations to investigate experimentally the top monolayer of a target. For example, if an energy selective detector is used at angles greater than 50° to the surface normal nearly all of the ejected atoms in the low-energy peak would arise only from the first layer.

Quantitative experimental measurements of the angular distribution of sputtered atoms from single crystal targets of copper are needed. Many of the older angular

distribution data were obtained under less than ideal conditions, and new data would do much to clarify the mechanisms responsible for low energy sputtering.

ACKNOWLEDGEMENTS

Special thanks are extended to Mr. Dick Bednar of the CSU-Fullerton computer center for many hours of patient assistance during the development of the SPUT1 program. We also thank Mr. Gene Dippel, director of the CSUF computer center, for facilitating our use of the State University Data Center CYBER-730/760 system.

REFERENCES

1. M. F. Dumke, Ph.D. Thesis, California Institute of Technology (1982).
2. M. F. Dumke, T. A. Tombrello, R. A. Weller, R. M. Housley, and E. H. Cirlin, *Surface Science* **124,** 407 (1983).
3. D. E. Harrison, Jr., *J. Appl. Phys.* **52,** 1499 (1981).
4. D. E. Harrison, Jr. and R. P. Webb, *J. Appl. Phys.* **53,** 4193 (1982).
5. G. D. Magnuson and C. E. Carlston, *J. Appl. Phys.* **34,** 3267 (1963).
6. A. L. Southern, W. R. Willis, and M. T. Robinson, *J. Appl. Phys.* **34,** 153 (1963).
7. D. E. Harrison, Jr., *Radiation Effects* **70,** 1 (1983).
8. D. E. Harrison, Jr., P. W. Kelly, B. J. Garrison, and N. Winograd, *Surface Science* **76,** 311 (1978).
9. D. E. Harrison, Jr., N. S. Levy, J. P. Johnson, III, and H. M. Effron, *J. Appl. Phys.* **39,** 3742 (1968).
10. D. E. Harrison, Jr., W. L. Gay, and H. M. Effron, *J. Math. Phys.* **10,** 1179 (1969).
11. M. H. Shapiro, Technical Report BB-1, California Institute of Technology.
12. B. J. Garrison, N. Winograd, and D. E. Harrison, Jr., *Phys. Rev.* **B18,** 6000 (1978).
13. D. E. Harrison, Jr., C. E. Carlston, and G. D. Magnuson, *Phys. Rev.* **139,** A737 (1965).
14. D. E. Harrison, Jr., *Proceedings of the Symposium on Sputtering*, P. Varga, G. Betz and F. P. Viehbock (Eds.) (Perchtoldsdorf/Vienna, 1980), p. 36.
15. M. W. Thompson, *Physics Reports* **69,** 337 (1981).
16. B. W. Farmery and M. W. Thompson, *Phil. Mag.* **18,** 415 (1968).
17. D. P. Jackson, *Radiation Effects* **18,** 185 (1973).
18. M. T. Robinson, in *Sputtering by Particle Bombardment I,* R. Behrisch (Ed.) (Springer-Verlag, 1981), p. 73.
19. D. E. Harrison, Jr. and C. B. Delaplain, *J. Appl. Phys.* **47,** 2255 (1976).